Review

Recent Progress in the Integration of CO$_2$ Capture and Utilization

Huanghao Ning [1,2], Yongdan Li [1,2,3] and Cuijuan Zhang [1,2,*]

[1] Tianjin Key Laboratory of Applied Catalysis Science and Technology, State Key Laboratory of Chemical Engineering, School of Chemical Engineering and Technology, Tianjin University, Tianjin 300072, China; hhning@tju.edu.cn (H.N.); yongdan.li@aalto.fi (Y.L.)

[2] Collaborative Innovation Center of Chemical Science and Engineering (Tianjin), Tianjin 300072, China

[3] Department of Chemical and Metallurgical Engineering, School of Chemical Engineering, Aalto University, Kemistintie 1, P.O. Box 16100, FI-00076 Espoo, Finland

[*] Correspondence: cjzhang@tju.edu.cn

Abstract: CO$_2$ emission is deemed to be mainly responsible for global warming. To reduce CO$_2$ emissions into the atmosphere and to use it as a carbon source, CO$_2$ capture and its conversion into valuable chemicals is greatly desirable. To reduce the transportation cost, the integration of the capture and utilization processes is a feasible option. Here, the recent progress in the integration of CO$_2$ capture and conversion is reviewed. The absorption, adsorption, and electrochemical separation capture processes integrated with several utilization processes, such as CO$_2$ hydrogenation, reverse water–gas shift reaction, or dry methane reforming, is discussed in detail. The integration of capture and conversion over dual functional materials is also discussed. This review is aimed to encourage more efforts devoted to the integration of CO$_2$ capture and utilization, and thus contribute to carbon neutrality around the world.

Keywords: carbon neutrality; CO$_2$ capture; CO$_2$ conversion; integration

1. Introduction

Carbon dioxide capture, utilization, and storage (CCUS) are increasingly gaining global attention. The challenge is to meet the energy demand while balancing CO$_2$ emissions. Several solutions have been proposed to reduce the CO$_2$ emission, namely, increasing the utilization of eco-friendly energy sources, such as wind and solar energy, to improve the energy efficiency. However, the advancement of such technologies is currently still limited and can be an optimal option in the long-term. At present times, the CCUS technology is more effective and can be a short-term alternative.

CO$_2$ can be captured using various technologies, such as amine absorption, porous materials adsorption and membrane separation. Since CO$_2$ itself is a carbon source, it can be converted into valuable chemicals via dry methane reforming (DMR), CO$_2$ hydrogenation, reverse water–gas shift reaction, etc. There are excellent reviews on both the technologies [1–3]. However, the traditional CO$_2$ capture and utilization processes are separated, which inevitably increases the transportation cost. To reduce or even eliminate such cost, the integration of CO$_2$ capture and utilization is greatly desirable. This review focuses on the integration of CO$_2$ capture and utilization. The relevant processes and the materials involved will be discussed.

2. Integration of CO$_2$ Capture and Utilization

Integrated CO$_2$ capture and utilization aims to capture CO$_2$ from gas streams and other emission sources and convert it into valuable chemicals or energy sources. The key is to find the match between the CO$_2$ separation process and the CO$_2$ utilization process, including the temperature and pressure, etc.

2.1. Integration of CO_2 Absorption and Conversion

CO_2 can be captured via physical or chemical absorption depending on the interaction between CO_2 and the absorbent. The former mainly utilizes the solubility of each gas component in the solvent whereas the latter involves chemical reactions between CO_2 and the absorbent. Chemical absorption is mostly employed with organic amine, hot potash, and liquid ammonia solvents considering its easy operation and mild working conditions [4]. Accordingly, it can be integrated with CO_2 hydrogenation for the production of formic acid or methanol.

Amine-based CO_2 capture and conversion integrated reactors consist of a series of amine sorbents and metal ions that form a pincer complex, such as pincerpentaethylene-hexamine (PEHA), pyrrolizidine, N,N,N′,N″,N″-pentamethyldiethylenetriamine (PMDTA) and polyethyleneimine (PEI). These are coupled with metal pincer-based homogeneous catalysts [5–8]. Due to the presence of multiple amine sites [9], PEI can be used as a superior CO_2 absorber [10], which can absorb both high and low concentrations of CO_2 [11]. Li et al. [12] used $PEI/RhCl_3 \cdot 3H_2O/CyPPh_2$ to capture CO_2 and convert it in situ (Figure 1a). PEI absorbs CO_2 from air in an ethylene glycol solution containing PEI and converts it into amino formate esters and alkyl carbonate esters. CO_2 is hydrogenated in situ to form formate salts (TON = 260) in the presence of $RhCl_3$-$3H_2O/CyPPh_2$, demonstrating the first in situ CO_2 capture and conversion to formate. Multifunctional materials can be synthesized by modifying the PEI backbone with iminophosphine ligand functionality and subsequently metallizing it with Ir precursors. About 65% of the available primary amines on PEI can be modified to form iminophosphine/Ir (PN/Ir) for balanced CO_2 capture and conversion, resulting in higher formic acid yields. PEI with relatively lower molecular weight has better CO_2 capture ability and catalytic activity (Figure 1b) [13]. Kothandaraman et al. [14] reported, for the first time, a green and simplified method for in situ conversion of captured CO_2 to formate in aqueous media in the presence of Ru- and Fe-based pincer complexes without excess alkali, with yields of up to 95% of the formate.

In addition to formate, the captured CO_2 can be converted into methanol. In 2015, Rezayee et al. [15] prepared methanol by tandem CO_2 capture and in situ conversion of dimethylamine with homogeneous ruthenium complexes under basic conditions. Dimethylamine can react with CO_2 and inhibit the formation of formic acid. The conversion of CO_2 is >95% (Figure 1c). Moreover, Kothandaraman et al. [5] first proposed and demonstrated a system for capturing CO_2 from air (~400 ppm) and converting it in situ (Figure 1d), which consisted of PEHA and Ru–PNP complex, with a methanol yield of 79%. Integrated systems for CO_2 capture and conversion into methanol are still uncommon. The major obstacle is the harsh reaction conditions to produce methanol, which involves a high-pressure gas-phase catalyst reactor at relatively low temperatures of 200–300 °C and high pressures of 50–100 atm.

The amine-based materials offer the potential to capture and convert CO_2 under mild conditions. Due to the relatively high CO_2 capture capacity of PEI, it can directly capture CO_2 from the air, which also removes the limitation of constructing CO_2 capture equipment. However, the high selectivity of some materials to carbon dioxide poses a challenge for the regeneration of amines. Furthermore, the toxicity and corrosiveness of amine solvents limit their industrial application. To drive future research, it is essential to explore systems that are highly efficient and recyclable, enabling CCU to establish a reliable foundation for industrial applications.

2.2. CO_2 Adsorption and Conversion Integration

Similar to absorption, adsorption separation can also be divided into chemisorption and physisorption according to the interaction between CO_2 and the adsorbate, with the former forming covalent bonds whilst the latter forms bond with electrostatic attraction and van der Waals forces. Here, we mainly focus on the physisorption and the subsequent utilization of CO_2.
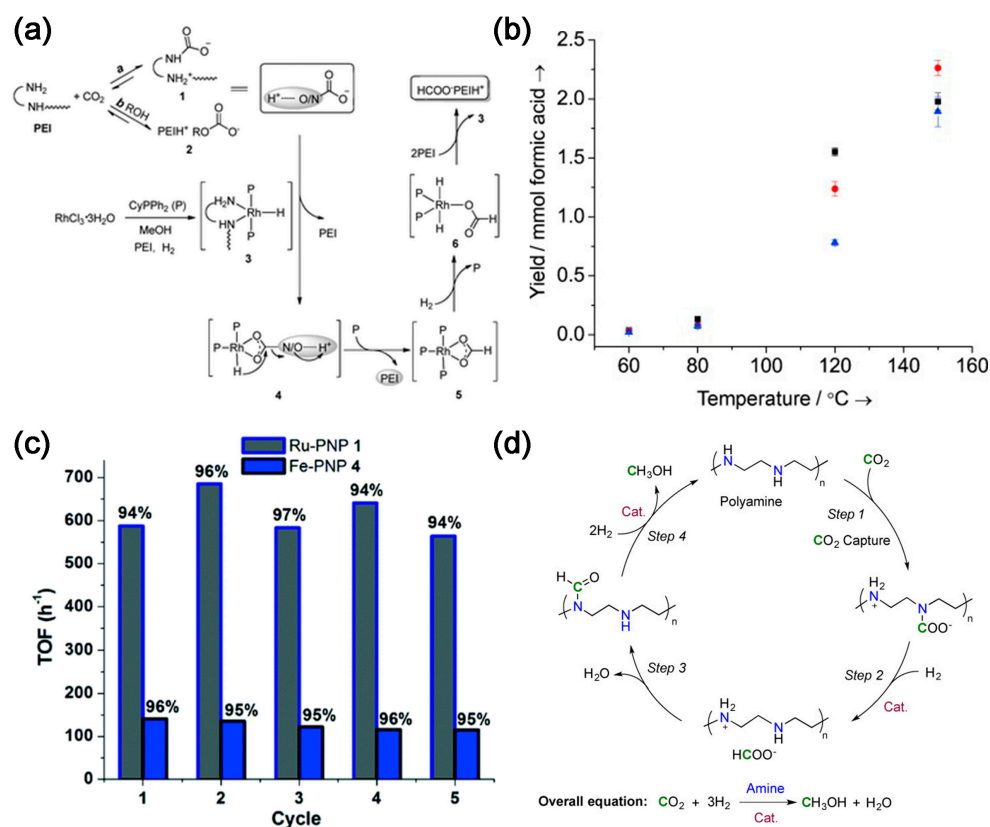
Figure 1. (**a**) Proposed pathways of carbon capture and subsequent hydrogenation of the captured CO_2 [12]; (**b**) Formic acid yields in the hydrogenation of CO_2 catalyzed by the PEI–PN/Ir materials as a function of temperature and MW of PEI for PEI_{600}–PN/Ir (▪), PEI_{1800}–PN/Ir (●), and $PEI_{25\,000}$–PN/Ir (▲) [13]. (**c**) Multiple recycling of the catalyst in biphasic reaction mixture. Yield (%) of formate is relative to the amount of CO_2 captured. Ru–PNP 1: Cat 1 = 10 μmol, T = 55 °C, H_2 = 50 bar, 17.2 mmol diazabicyclo[2.2.2]octane (DABCO) + 3 mL H_2O (CO_2 captured each cycle = 15 mmol), 3 mL additional H_2O–4 mL 2-Methyltetrahydrofuran (2–MeTHF) added for hydrogenation study. Fe–PNP 4: Cat 4 = 20 μmol, T = 55 °C, H_2 = 50 bar, 17.2 mmol DABCO + 3 mL H_2O (CO_2 captured each cycle = 15 mmol), 3 mL additional H_2O–4 mL 2–MeTHF added for hydrogenation study [14]. (**d**) Proposed reaction sequence for CO_2 capture and in situ hydrogenation to CH_3OH using a polyamine [5].

Porous organic polymers (POPs) are a series of new two- or three-dimensional networked polymeric materials formed by covalent bonding of organic small molecule substrates through specific chemical reactions, usually with microporous, mesoporous or multistage pore structures. They have promising applications in separation, sensor and catalysis [16]. The ionic porous organic polymers (IPOPs) are generally classified as porous organic materials, whose backbone typically includes anions or cations. They can be divided into IPOPs with cationic moieties, IPOPs with anionic moieties, and IPOPs with zwitterionic moieties. Common cationic moieties include imidazolium, pyridinium, viologen, and quaternary phosphonium, whereas more common anionic moieties include tetrakis(phenyl)borate and tris(catecholate) phosphate. The inclusion of these ionic moieties in porous materials can enhance their CO_2 capture capacity and catalyze the in situ CO_2 conversion.

In 2011, tetrakis(4-ethynylphenyl)methane and diiodoimidazolium salts were used to prepare tubular microporous organic via Sonogashira coupling reaction networks bearing imidazolium salts (T-IM) (Figure 2a). The material, with a microporous structure of specific surface area (620 $m^2\ g^{-1}$), shows good catalytic activity towards the conversion of CO_2 to cyclic carbonates [17]. Wang et al. [18] utilized the Friedel–Crafts reaction to synthesize

imidazole-based IPOPs. The specific surface area can reach up to 926 m^2 g^{-1}; however, its CO_2 capture capacity is only 14.2 wt%. Nevertheless, the polymer exhibits good stability and repeatability. Sun et al. [19] demonstrated, for the first time, the capture and in situ conversion of CO_2 into cyclic carbonates under relatively mild room temperature conditions using a metal-free solvent followed by a heterogeneous catalytic system. The effect of halogen anions (Cl, Br, and I) and quaternary phosphonium cations on the catalytic activity was investigated. The catalytic activity follows the order Cl$^-$ > Br$^-$ > I$^-$ (Figure 2b), because the rate-controlling step of the reaction is ring opening by anion attack on the epoxide [20].
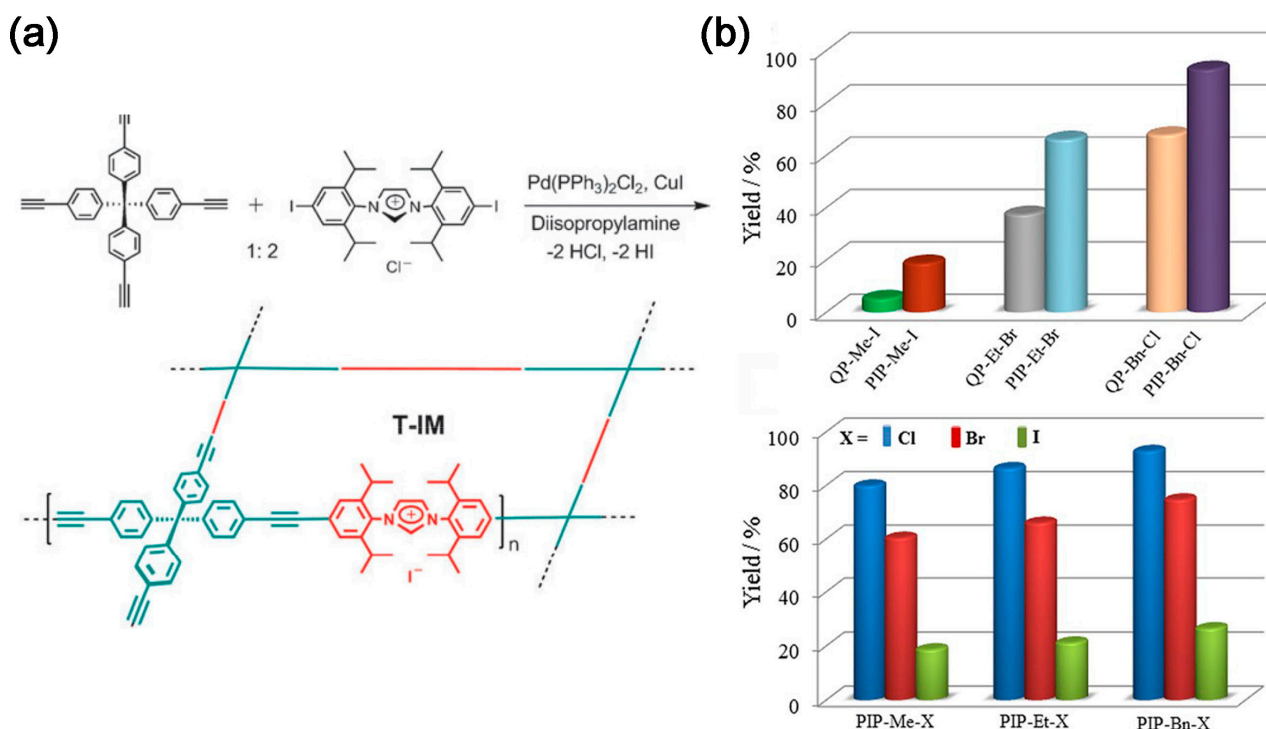

Figure 2. (**a**) Preparation of porous organic networks bearing imidazolium salts [17]; (**b**) Yields of chloropropene carbonate from the cycloaddition of epichlorohydrin and CO_2 catalyzed by PIPs with corresponding QPs and PIP-Me-X, PIP-Et-X, and PIP-Bn-X (X = Cl, Br, and I). Reaction conditions: epichlorohydrin (1.0 g, 10.9 mmol), catalyst (0.05 mmol, based upon the quaternary phosphonium salt), 323 K, CO_2 (ambient pressure), and 24 h [19].

In addition to IPOP, the porphyrin-based organic polymer (POP-TPP) can also be used. Xiao et al. [21] synthesized a hierarchically porous organic polymer (POP-TPP) by polymerizing vinyl-functionalized tetraphenylporphyrin monomer, and then metalated it with different metals (Co^{3+}, Zn^{2+}, and Mg^{2+}). The resulting heterogeneous catalysts have rich active sites and exhibit higher activity than the homogenous Co/TPP catalyst at relatively low CO_2 concentrations, primarily due to the favorable enrichment of CO_2 in the porous structure (micropores and nanochannels) of Co/POP-TPP. The TOF of the catalysts decreases in the following order: Co/POP-TPP (436 h^{-1}) > Zn/POP-TPP (326 h^{-1}) > Mg/POP-TPP (171 h^{-1}) (Table 1). Later, a series of high surface area hollow tubular metal (Al, Co, Fe, and Mn) porphyrin-based hypercrosslinked polymers (HCP) were synthesized via Friedel–Crafts alkylation reactions. Al-HCP can catalyze the formation of propylene carbonate with a selectivity of approximately 99% after only 1 h with 2.0 mol% TBAB catalyst [22].

Table 1. Cycloaddition of epichlorohydrin with CO_2 to form cyclic carbonate over various catalysts at 29 °C [21].

Entry	Catalysts	Additives	Time (h)	Conv. (%) [a]	Select. (%) [a]
1 [b]	POP-TPP	n-Bu$_4$NBr	24	52.1	>99.0
2 [c]	Co/POP-TPP	n-Bu$_4$NBr	24	95.6	99
3 [c]	Co/TPP	n-Bu$_4$NBr	24	97.5	99
4	Co/POP-TPP	None	24	9.7	99
5	Co/TPP	None	24	18.5	99
6	None	n-Bu$_4$NBr	24	34	99
7 [d]	Co/POP-TPP	n-Bu$_4$NBr	96	96.1	99
8 [e]	Co/POP-TPP	n-Bu$_4$NBr	24	88.9	99
9 [f]	Zn/POP-TPP	n-Bu$_4$NBr	24	93.2	>99.0
10 [f]	Zn/TPP	n-Bu$_4$NBr	24	93.5	>99.0
11 [g]	Mg/POP-TPP	n-Bu$_4$NBr	24	80.5	>99.0
12 [g]	Mg/TPP	n-Bu$_4$NBr	24	99.3	>99.0
13 [h]	Co/POP-TPP	n-Bu$_4$NBr	24	93.6	99

Note: [a] Determined using GC analysis. [b] 48 mg of POP-TPP was used. [c] 50 mg of Co/POP-TPP (1.6 mg Co) or 19 mg of Co/TPP (1.6 mg Co) was used. [d] Co/POP-TPP catalyst (12.5 mg, 0.4 mg Co). [e] 50 mg of n-Bu$_4$NBr. [f] 50 mg of Zn/POP-TPP (2.3 mg Zn) or 23.5 mg of Zn/TPP (2.3 mg Zn) was used. [g] 50 mg of Mg/POP-TPP (1.4 mg Mg) or 37.0 mg of Mg/TPP (1.4 mg Mg) was used. [h] Recycled for 18 times.

Metal–organic frameworks (MOFs) are porous crystalline materials formed by coordination between metal ions or metal clusters and organic ligands, which are characterized by high porosity, high surface area, tunable pore size and geometric configuration, and functionalizable pore surface [23]. Consequently, they can be employed for CO_2 capture and utilization. The imidazolium-based poly(ionic liquid)s (denoted as polyILs) and ortho-divinylbenzene were used as cross-linking agents to polymerize in the pores of MIL-101 (Figure 3a), resulting in polyILs@MIL-101 materials with dual functions of CO_2 capture and conversion [24]. For MOFs materials, ordered nanochannels can effectively promote the enrichment of CO_2 at the active sites and accelerate the CO_2 conversion; Lewis basic sites (LBSs) can supply electrons to activate CO_2 [25,26]. In order to restore the real CO_2 capture process, a CO_2 capture and in situ conversion system was designed by simulating the flue gas feed, where the lanthanide (III) complex of 1-vinylimidazole (Vim) was immobilized with DUT-5 by a combination of ligand and in situ polymerization (Figure 3b). This work opens up a general pathway for future research and validates the effectiveness of MOFs for practical applications in CO_2 capture and conversion [27].

Although the integrated materials have demonstrated good CO_2 capture and enrichment capabilities, their performance under the real industrial exhaust emissions that contain acidic gases, such as SO_x, NO_x, and steam, remain to be explored.

2.3. CO_2 Electrochemical Membrane Separation and Conversion Integration

Electrochemical membrane separation is a technology that achieves gas separation through electrochemical reaction. The membrane can be mixed oxide ion-carbonate conductor (MOCC), such as $Y_{0.16}Zr_{0.84}O_{2-\delta}$-molten carbonate (YSZ-MC), $Ce_{0.8}Sm_{0.2}O_{1.9}$-MC (SDC-MC), $Ce_{0.9}Gd_{0.2}O_{1.9}$-MC (GDC-MC), and $Bi_{1.5}Y_{0.3}Sm_{0.2}O_{3-\delta}$-MC (BYS-MC); mixed electron-carbonate conductor (MECC), such as stainless steel-MC (SS-MC), Ag-MC, and Ni-MC; or mixed oxide ion-electron-carbonate conductor (MOECC), such as $La_{0.6}Sr_{0.4}Co_{0.8}Fe_{0.2}O_{3-\delta}$-MC (LSCF-MC), $La_{0.5}Sr_{0.5}Fe_{0.8}Cu_{0.2}O_{3-\delta}$-MC (LSFCu-MC) and NiO-SDC-MC based on the charge carriers [2]. Generally, the carbonates (Li-Na-K-based) show high electrical conductivity and low viscosity only at relatively high temperature, e.g., >600 °C. Accordingly, it can be well integrated with the high temperature CO_2 utilization processes, such as DMR and reverse water–gas shift (RWGS) (Table 2).
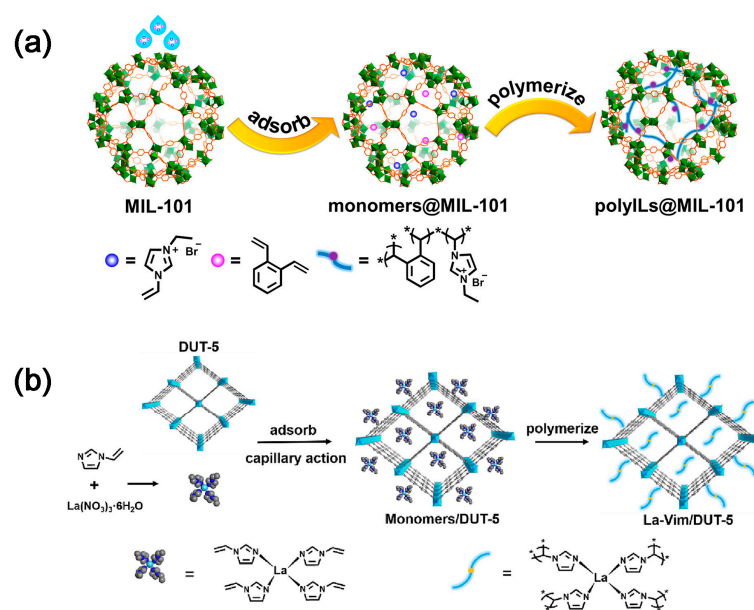
Figure 3. Schematic illustration of the preparation of (**a**) polyILs@MIL–101 [24] and (**b**) La–Vim/DUT–5 [27]. The "*" represents the monomer in the polymer.

Lin and co-workers first modeled the high temperature tube shell membrane reactor for separation and utilization of CO_2 from the flue gas and for simultaneous production of syngas using DMR. The membrane reactor is highly efficient for CCUS. The CH_4 conversion of 48.1% and an average CO_2 permeation flux of 1.52 mL cm^{-2} min^{-1} can be obtained at 800 °C with a 75 μm thick membrane and CH_4 space velocity of 3265 h^{-1} [28]. Later, Anderson et al. [29] experimentally studied the integration of CO_2 separation and DMR with LSCF-MC membrane and Ni/γ-alumina catalyst. The CO_2 permeation rate above 750 °C matches the reaction rate of DMR catalyst, and the order of syngas production activity is blank system < LSCF combustion catalyst < Ni/γ-alumina reforming catalyst. The conversion of CO_2 and CH_4 is 88.5 and 8.1%, respectively, generating a syngas H_2:CO ratio of about 1 [30]. To improve the performance, Zhang et al. [31] employed MOCC membrane (GDC-MC) (Figure 4a), and NMP (Ni-MgO-1 wt% Pt) and LNF (LaNi$_{0.6}$Fe$_{0.4}$O$_{3-\delta}$) catalysts. The yield of H_2 and CO and the conversion of CH_4 in the reactor with NMP catalyst is higher than that with LNF catalyst (Figure 4b,c), while the reactor with LNF catalyst shows better anti-coking performance and no significant degradation within 200 h. In addition, Zhang et al. [32] investigated the MECC membrane reactor (Ag-MC) coupled with dry-oxy methane reforming (DOMR) over an NMP catalyst. The CH_4 conversion is >82% and is stable over 115 h at 800 °C (Figure 4d). Similar reactor models can be applied to integrate CO_2 separation and oxidative dehydrogenation of ethane (ODHE) to prepare ethylene [33]. CO_2 can react with H_2 to make the reaction of ethane dehydrogenation forward, which can increase the selectivity of O_2-ODHE to produce ethylene [33].

The coupling of a dual-phase membrane reactor with a RWGS reaction was first reported by Chen et al. [34] to capture CO_2 and produce CO. Under a sweep gas condition of 1% H_2/He, the CO selectivity over LaNiO$_3$ (LNO) catalyst is >96% at 550–750 °C. Additionally, La$_{0.9}$Ce$_{0.1}$NiO$_{3-\delta}$ (LCNO) catalyst displays almost 100% CO selectivity and good thermal stability. The introduction of H_2 during the purge test enhances the permeation of CO_2. H_2O in dual-phase membrane systems can reduce the activation energy, possibly due to the conduction of hydroxide ions through the membrane [35].

The dual-phase membrane reactor can also increase the H_2 yield by removing CO_2. The concept of CO_2 removal was first applied to the steam reforming of methane reaction (SMR) to produce high concentration of H_2 by Wu et al. [36]. The asymmetric BYS-SDC-MC membrane reactor can convert methane into hydrogen via SMR reaction while simultaneously removing CO_2 to achieve a high concentration of hydrogen, with 84% CO_2 recovery

(Figure 5a). The results of the mathematical model (Figure 5b) demonstrate that CO_2 recovery from SMR in the CO_2 permeated membrane reactor exceeds 99% and a pure H_2 gas stream without CO gas can be achieved [37].
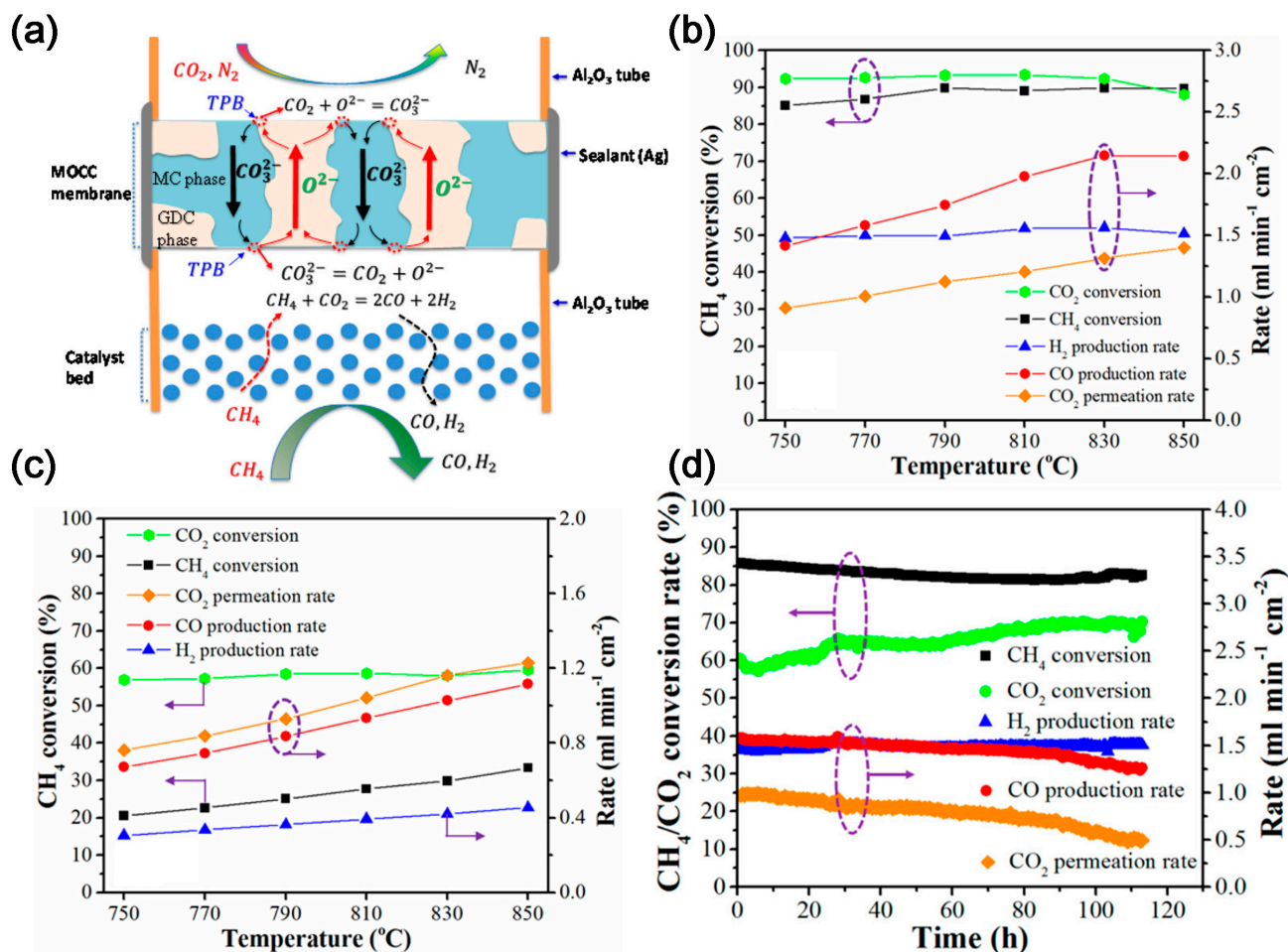

Figure 4. (**a**) Schematic illustration of a MOCC membrane reactor with a catalyst bed for electrochemical CO_2 capture and catalytic DMR. TPB: triple phase boundary [31]. (**b**) Effect of temperature on the DMR performance of a GDC–MC membrane reactor with an NMP catalyst [31]. (**c**) Effect of temperature on the DMR performance of a GDC–MC membrane reactor with an NMP catalyst and an LNF catalyst [31]. (**d**) Stability of DOMR performance of the Ag–MC MECC membrane reactor at 800 °C with NMP catalyst. Feed gas: 75 mL min^{-1} N_2, 15 mL min^{-1} CO_2, and 10 mL min^{-1} O_2; sweep gas: 0.94 mL min^{-1} CH_4 and 50 mL min^{-1} Ar [32]. The dotted circles and arrows in the figure represent the axes corresponding to the curve.

The dual-phase membrane reactors can also be utilized for the oxidative coupling of methane (OCM) reaction. The high oxygen partial pressure in conventional OCM reactors often results in low C_2 selectivity. Li et al. [38] combined CO_2/O_2 transport membrane (CTM) and OCM reaction to build a new membrane reactor model (Figure 5c), which shows higher conversion of CH_4 than the traditional fixed-bed reactor model and better coking resistance. Based on this, Zhang et al. [39] developed a membrane reactor combining SDC-NiO-MC and 2%Mn–5%Na_2WO_4/SiO_2 catalyst. The co-captured CO_2/O_2 mixture converts CH_4 into C_2H_6 over the 2%Mn–5%Na_2WO_4/SiO_2 catalyst, followed by thermal cracking into C_2H_4 and H_2. In the presence of CO_2, the O_2 partial pressure is reduced, thereby reducing the possibility of re-oxidation of C_2 products, which leads to a higher C_2 selectivity.
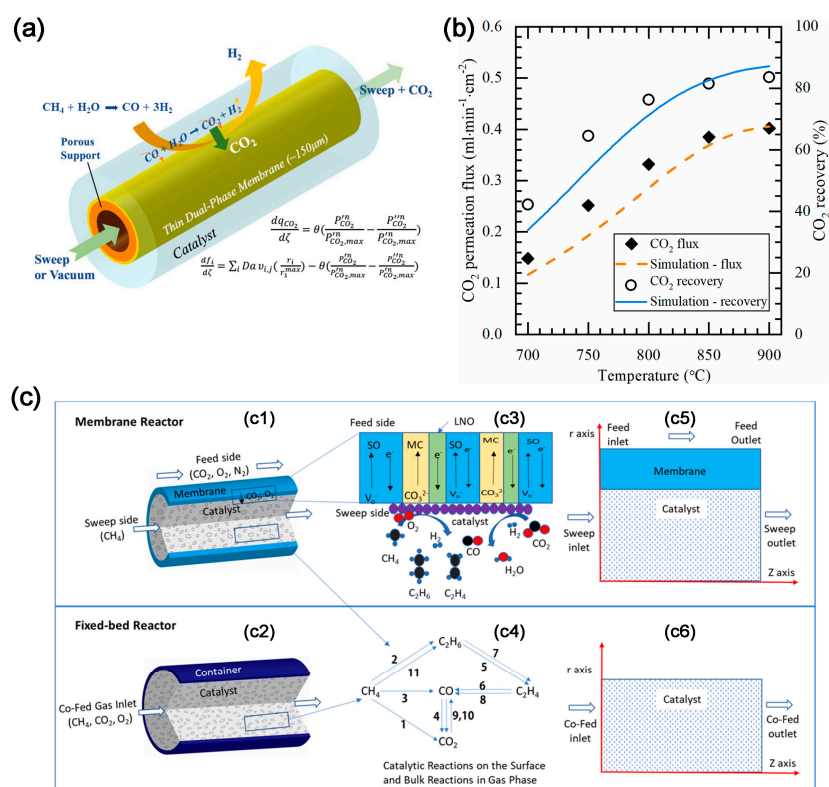
Figure 5. (**a**) Schematic illustration of membrane reactor [37]. (**b**) Comparison of CO$_2$ flux and recovery of the membrane reactor between experimental results and modeling results. Conditions: sweep: He = 200 mL min^{-1}; feed: CH$_4$ = 5 mL min^{-1}; S/C = 3; both sides of the membrane were at 1 atm [37]. (**c**) Schematic illustration of (**c1**) Membrane reactor; (**c2**) Co-fed fixed bed reactor; (**c3**) Charge species transport and surface reactions in the membrane reactor; (**c4**) Reaction pathway diagram. 2D axial symmetric computational domain of (**c5**) Membrane reactor; (**c6**) Co-fed fixed bed reactor [38].

Table 2. Summary of electrochemical membrane materials integrated reactors.

Membrane	Catalyst	Reaction	Ref.
La$_{0.6}$Sr$_{0.4}$Co$_{0.8}$Fe$_{0.2}$O$_{3-\delta}$ Li-Na-K	10 wt%Ni-/γ-Al$_2$O$_3$	DMR	[29]
Ce$_{0.8}$Gd$_{0.2}$O$_{1.9}$ Li-Na	Ni-MgO-1 wt% Pt LaNi$_{0.6}$Fe$_{0.4}$O$_{3-\delta}$	DMR	[31]
Ag Li-Na	Ni-MgO-1 wt% Pt	DOMR	[32]
NiO-SDC Li-Na	Ni-MgO-1 wt% Pt	DOMR	[40]
Ce$_{0.8}$Gd$_{0.2}$O$_{1.9}$ Li-Na	5 wt% Cr$_2$O$_3$- ZSM-5	Ethane-to-Ethylene	[33]
Ce$_{0.9}$Pr$_{0.1}$O$_{2-\delta}$-Pr$_{0.6}$Sr$_{0.4}$Fe$_{0.5}$Co$_{0.5}$O$_{3-\delta}$ Li-Na-K	10 wt%Ni-/γ-Al$_2$O$_3$	DOMR	[41]
LNO/SDC Li-Na	LNO/LCNO	RWGS	[34]
BYS-SDC Li-Na-K	Ni-based catalyst (HiFUEL R110)	SMR	[36]
γ-LiAlO$_2$-Ag Li-Na-K	γ-LiAlO$_2$-Ag	Syngas production	[42]
NiO-SDC Li-Na	2%Mn-5%Na$_2$WO$_4$/SiO$_2$	OCM	[39]

Note: Li-Na-K = Li$_2$CO$_3$: Na$_2$CO$_3$:K$_2$CO$_3$ with ratio of 42.5:32.5:25 mol%; Li-Na = Li$_2$CO$_3$: Na$_2$CO$_3$ with ratio of 52:48 mol%.

2.4. CO₂ Capture and Conversion over Dual-Function Materials (DFMs)

Inorganic metal dual-functional materials (DFMs) combine the capture and conversion of CO_2 into organic compounds. DFMs consist of the CO_2 absorption component and the catalytic CO_2 conversion component. The former is usually composed of alkali metal oxides or carbonates whilst the latter comprises metal-based catalysts, such as Ru, Rh, and Ni for DMR, dry ethane reforming (DER), RWGS reaction, and CO_2 methanation [43–45]. Those processes can be well integrated with CO_2 absorption considering their similar operating temperatures.

In 2018, Kim et al. [46] proposed and demonstrated the feasibility of using DFM to capture CO_2 and convert it in situ with renewable CaO as an absorber of CO_2 and Ni/MgO-Al₂O₃ as a catalyst for DMR. The concentration of CO_2 in the exhaust gas is less than 0.08%, and the ratio of H_2 to CO is 1.06. Tian et al. [47] synthesized CaO-Ni DFM using a sol–gel method. The ratio of H_2 to CO is 1.1, which is similar to Kim's results [46]. Methane decomposition can occur simultaneously during the reaction. The deposited carbon facilitates the reaction of CO_2 with CaO-Ni; the CH_4 conversion rate can reach 86%. Compared to other processes for DMR, the in situ consumption of CO_2 on the catalyst surface promotes a positive shift of equilibrium in favor of $CaCO_3$ decomposition, which allows the otherwise energy-intensive calcium cycling process to proceed at lower temperatures, thus further alleviating the deactivation problem during calcination. The energy consumed is 22% lower than the conventional consumption. In order to improve the activity and stability of Ni-CaO in the DMR reaction [48], CeO_2 was added to the support, with a Ca:Ce molar ratio of 85:15. The resultant catalyst demonstrates good stability and maintains ≈ 80–90% activity over nine cycles at 650 °C, which is over two times better than the material without CeO_2 modification (Figure 6a). The dispersion of Ni and the reducibility of NiO are improved, enhancing the DMR activity. Due to the high mobility of lattice oxygen in CeO_2, the CeO_2 modification can inhibit the accumulation of non-active carbon on Ni.
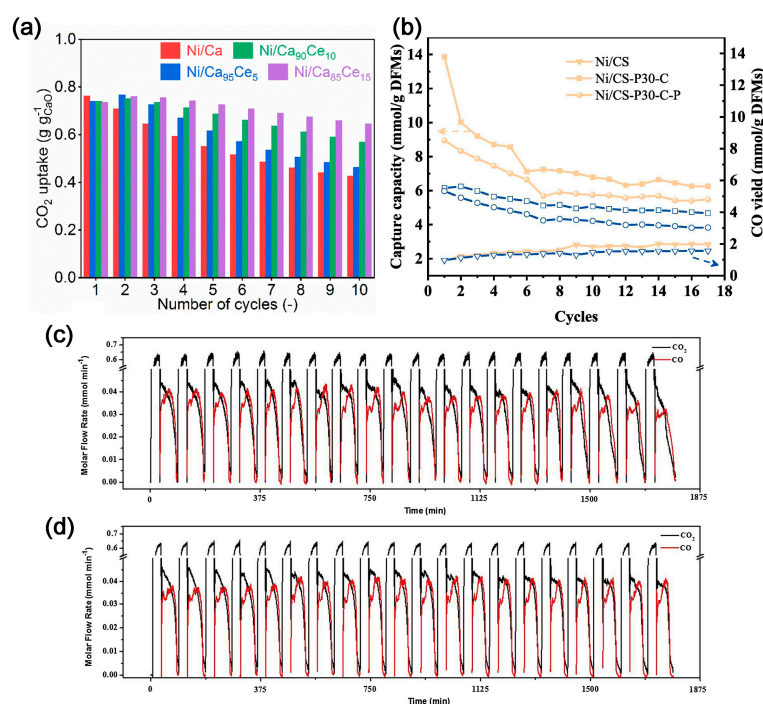

Figure 6. (**a**) Comparison of cyclic CO_2 capture-release stability of the as-prepared bifunctional materials at 650 °C [48]. (**b**) CO_2 sorption capacities and CO productivities of Ni/CS, Ni/CS–P30–C and Ni/CS-P30-C-P at 650 °C within 17 cycles [49] (The symbols indicate different preparation methods. The yellow and blue lines represent CO_2 sorption capacities and CO productivities, respectively). Cyclic CO_2 capture and conversion reactions of (**c**) $Ca_1Ni_{0.1}$; and (**d**) $Ca_1Ni_{0.1}Ce_{0.033}$ [50].

In addition to DMR, the captured CO_2 can be also converted into methane over DFM (Table 3). The Farrauto group is a pioneer in the study of CO_2-Met DFM. They prepared DFM using Ru as the metal catalyst, CaO as the CO_2 absorbent, and γ-Al_2O_3 as a carrier [51]. At 320 °C and 10% CO_2/N_2, CO_2 capture was carried out followed by methane production reaction for 2 h with 4% H_2/N_2. The 5% Ru-10% CaO/γ-Al_2O_3 exhibits the highest activity. In the CO_2 capture cycle test with presence of steam, the purity of obtained methane can reach up to 99%. Duyar et al. [52,53] synthesized Ru- and Rh-based DFM from the nitrates of Ru and Rh, respectively, via impregnation. The Rh-based DFMs show better activity. However, their high cost limits large-scale application. In order to reduce the cost, Bermejo-Lopez et al. studied DFMs using Ni as the catalyst [54,55]. Ni-CaO/γ-Al_2O_3 and Ni-Na_2CO_3/γ-Al_2O_3 with different Ni loadings were synthesized via impregnation. The methane yield of 10% Ni-Na_2CO_3/γ-Al_2O_3 is 186 μmol CH_4 g^{-1} at 400 °C and it is 142 μmol CH_4 g^{-1} at 520 °C for 15% Ni-CaO/γ-Al_2O_3. In addition, Al-Mamoori et al. [56] prepared DFMs using Ni-impregnated CaO- and MgO-based double salts as CO_2 absorber and catalyst, respectively, and γ-Al_2O_3 as the carrier. The CO_2 absorption was first saturated in a 10% CO_2/N_2 atmosphere at 650 °C and 1 bar, and then a 5% C_2H_6/N_2 mixture was passed into the reactor to react with CO_2. The Ni@(K-Ca)/γ-Al_2O_3 system exhibits the highest CO_2 absorption and 100% C_2H_6 conversion. Nevertheless, Ni usually requires high reduction temperature and is very sensitive to O_2 in the feed gas, and its long-term stability remains to be improved for the CO_2-Met reaction.

Table 3. Carbon dioxide methanation dual-functional materials summary.

DFM	Condition (°C)		Ref.
	Absorption	**Reaction**	
Ni-CaO/Al_2O_3	280–520 10% CO_2/Ar	280–520 10% H_2/Ar	[55]
Ni-Na_2CO_3/Al_2O_3	280–520 10% CO_2/Ar	280–520 10% H_2/Ar	
Ni-Na_2O/Al_2O_3	320 7.5% CO_2/N_2 and 7.5% CO_2, 4.5% O_2, 15% H_2O/N_2	320 15% H_2/N_2	[52]
Ru-Na_2O/γ-Al_2O_3	320 15% CO_2/N_2	320 20% H_2/N_2	[57]
Rh-CaO/γ-Al_2O_3	320 10% CO_2/N_2	320 2% H_2/N_2	
Ru-CaO/γ-Al_2O_3	280–400 1.4% CO_2/Ar and 11% CO_2/Ar	280–400 10% H_2/Ar	[54]
Ru-Na_2CO_3/γ-Al_2O_3	280–400 1.4% CO_2/Ar and 11% CO_2/A	280–400 10% H_2/Ar	
Ru-CaO/γ-Al_2O_3	320 10% CO_2/air and 8% CO_2/21% H_2O/air	320 5% H_2/N_2	[51]
Ru-CaO/γ-Al_2O_3	320 10% CO_2/N_2	320 4% H_2/N_2	[57]
Ru-CaO/γ-Al_2O_3	320 7.5% CO_2, 4.5% O_2, 15% H_2O/N_2	320 5% H_2/N_2	[58]
Ru-Na_2CO_3/γ-Al_2O_3	320 7.5% CO_2/N_2 and 7.5% CO_2, 4.5% O_2, 15% H_2O/N_2	320 5% H_2/N_2	[59]
Ru-Na_2O/γ-Al_2O_3	250–350 7.5% CO_2, 4.5% O_2, 15% H_2O/N_2	250–350 15% H_2/N_2	[60]

DFMs can also convert the captured CO_2 into valuable chemicals via RWGS reactions and ethane reforming. To investigate the effect of preparation methods on the performance of DFMs, Wang et al. [49] synthesized DFMs using three different methods, namely wet-mixing, acidification/impregnation, and acidification/impregnation combined with citric acid complexation. The Ni/CS-P30-C, prepared via acid pretreatment of carbide slag followed by citric acid complex, exhibits a high CO_2 sorption capacity (13.28 mmol g^{-1} DFMs) and a great CO productivity (5.12 mmol g^{-1} DFMs) at 650 °C, and also demonstrates better CO_2 capture and in situ conversion (Figure 6b). Sun et al. [50] investigated the effect of Ce loading onto the Ca-Ni-based DFM on the performance of CO_2 capture and RWGS. The DFM with Ca:Ni:Ce = 1:0.1:0.033 (molar ratio) exhibits high cycling stability, and 100% CO selectivity (Figure 6c,d). The addition of CeO_2 effectively prevents the growth and aggregation of NiO and CaO species.

The primary concerns are catalyst deactivation during the reaction, carbon deposition, and matching capture and conversion rates, along with the requirement of evaluating the life cycle and economics of the integrated system. Therefore, further research is necessary in the future on aspects, such as reaction atmosphere, temperature, life cycle, economic analysis, and industrial applications.

3. Conclusions, Challenges and Opportunities

In summary, the integration of CO_2 capture and utilization is reviewed, namely the absorption, adsorption, and electrochemical separation capture processes integrated with several utilization processes. Initially, it is imperative to ensure that the operational conditions of the CO_2 capture process and the subsequent reaction process are fundamentally congruent, encompassing factors, such as temperature, pressure, pH, and other relevant parameters. Subsequently, the CO_2 absorption materials can be more effectively combined with the catalyst without impeding their respective performances. The point is to find the match between the operating temperature of both processes. To improve the performance of the integration system, one of the key factors is to achieve the match between the capture rate and the conversion rate. For example, in the MOCC and DMR system, matching the CO_2 separation rate of the MOCC membrane and the conversion rate over DMR catalyst is crucial. Unfortunately, such studies are very limited. Of course, improving the performance (activity, and stability) of the single process, either the capture or the conversion process, is desirable.

Although the integration of CO_2 capture and conversion is very promising to lower the CO_2 concentration in the atmosphere, there are still many challenges ahead. The amine-based absorption is currently employed by the industry, however, their toxicity, corrosiveness and high cost limit their further market applications. Suitable amine-based or solid amine-based materials with low-energy, low-cost integrated CO_2 capture and conversion capabilities remain to be developed. For POP-based materials, their long-term and cycling stability, the impact of SO_x, NO_x, and other gases remain unclear. The production cost and complexity should be evaluated for future commercial promotion. The electrochemical membrane reactors integrated with catalysts is very promising for high-temperature CO_2 capture and conversion, but the CO_2 permeation flux and long-term stability are still needed to be improved. For the DFM-based materials, researching how to achieve the match between CO_2 capture and conversion is critical. The issues related with catalyst deactivation and operational life also remain to be solved.

To expedite innovation in the chemical industry, an integrated approach combining chemical experimentation with machine learning algorithms can be pursued. This paradigm shift will enable researchers to identify optimal materials faster and more efficiently, ultimately accelerating the pace of innovation in the global chemical industry.

References

1. Song, K.S.; Fritz, P.W.; Coskun, A. Porous organic polymers for CO_2 capture, separation and conversion. *Chem. Soc. Rev.* **2022**, *51*, 9831–9852. [CrossRef]
2. Zhang, P.; Tong, J.; Huang, K.; Zhu, X.; Yang, W. The current status of high temperature electrochemistry-based CO_2 transport membranes and reactors for direct CO_2 capture and conversion. *Prog. Energy Combust. Sci.* **2021**, *82*, 100888. [CrossRef]
3. Yamada, H. Amine-based capture of CO_2 for utilization and storage. *Polym. J.* **2021**, *53*, 93–102. [CrossRef]
4. Maina, J.W.; Pringle, J.M.; Razal, J.M.; Nunes, S.; Vega, L.; Gallucci, F.; Dumée, L.F. Strategies for integrated capture and conversion of CO_2 from dilute flue gases and the atmosphere. *ChemSusChem* **2021**, *14*, 1805–1820. [CrossRef] [PubMed]

5. Kothandaraman, J.; Goeppert, A.; Czaun, M.; Olah, G.A.; Prakash, G.S. Conversion of CO_2 from air into methanol using a polyamine and a homogeneous ruthenium catalyst. *J. Am. Chem. Soc.* **2016**, *138*, 778–781. [CrossRef] [PubMed]

6. Kar, S.; Goeppert, A.; Prakash, G.S. Combined CO_2 capture and hydrogenation to methanol: Amine immobilization enables easy recycling of active elements. *ChemSusChem* **2019**, *12*, 3172–3177. [CrossRef]

7. Hanusch, J.M.; Kerschgens, I.P.; Huber, F.; Neuburger, M.; Gademann, K. Pyrrolizidines for direct air capture and CO_2 conversion. *Chem. Commun.* **2019**, *55*, 949–952. [CrossRef]

8. Guan, C.; Pan, Y.; Ang, E.P.L.; Hu, J.; Yao, C.; Huang, M.-H.; Li, H.; Lai, Z.; Huang, K.-W. Conversion of CO_2 from air into formate using amines and phosphorus-nitrogen PN 3P-Ru (ii) pincer complexes. *Green Chem.* **2018**, *20*, 4201–4205. [CrossRef]

9. Tailor, R.; Abboud, M.; Sayari, A. Supported polytertiary amines: Highly efficient and selective SO_2 adsorbents. *Environ. Sci. Technol.* **2014**, *48*, 2025–2034. [CrossRef]

10. Yang, S.; Zhan, L.; Xu, X.; Wang, Y.; Ling, L.; Feng, X. Graphene-based porous silica sheets impregnated with polyethyleneimine for superior CO_2 capture. *Adv. Mater.* **2013**, *25*, 2130–2134. [CrossRef]

11. Goeppert, A.; Czaun, M.; May, R.B.; Prakash, G.S.; Olah, G.A.; Narayanan, S. Carbon dioxide capture from the air using a polyamine based regenerable solid adsorbent. *J. Am. Chem. Soc.* **2011**, *133*, 20164–20167. [CrossRef]

12. Li, Y.-N.; He, L.-N.; Liu, A.-H.; Lang, X.-D.; Yang, Z.-Z.; Yu, B.; Luan, C.-R. In situ hydrogenation of captured CO_2 to formate with polyethyleneimine and Rh/monophosphine system. *Green Chem.* **2013**, *15*, 2825–2829. [CrossRef]

13. McNamara, N.D.; Hicks, J.C. CO_2 capture and conversion with a multifunctional polyethyleneimine-tethered iminophosphine iridium catalyst/adsorbent. *ChemSusChem* **2014**, *7*, 1114–1124. [CrossRef] [PubMed]

14. Kothandaraman, J.; Goeppert, A.; Czaun, M.; Olah, G.A.; Prakash, G.S. CO_2 capture by amines in aqueous media and its subsequent conversion to formate with reusable ruthenium and iron catalysts. *Green Chem.* **2016**, *18*, 5831–5838. [CrossRef]

15. Rezayee, N.M.; Huff, C.A.; Sanford, M.S. Tandem amine and ruthenium-catalyzed hydrogenation of CO_2 to methanol. *J. Am. Chem. Soc.* **2015**, *137*, 1028–1031. [CrossRef] [PubMed]

16. Zhang, T.; Xing, G.; Chen, W.; Chen, L. Porous organic polymers: A promising platform for efficient photocatalysis. *Mater. Chem. Front.* **2020**, *4*, 332–353. [CrossRef]

17. Cho, H.C.; Lee, H.S.; Chun, J.; Lee, S.M.; Kim, H.J.; Son, S.U. Tubular microporous organic networks bearing imidazolium salts and their catalytic CO_2 conversion to cyclic carbonates. *Chem. Commun.* **2011**, *47*, 917–919. [CrossRef]

18. Wang, J.; Sng, W.; Yi, G.; Zhang, Y. Imidazolium salt-modified porous hypercrosslinked polymers for synergistic CO_2 capture and conversion. *Chem. Commun.* **2015**, *51*, 12076–12079. [CrossRef]

19. Sun, Q.; Jin, Y.; Aguila, B.; Meng, X.; Ma, S.; Xiao, F.S. Porous ionic polymers as a robust and efficient platform for capture and chemical fixation of atmospheric CO_2. *ChemSusChem* **2017**, *10*, 1160–1165.

20. Smith, J.G. *Organic Chemistry*, 3rd ed.; McGraw-Hill: Singapore, 2011.

21. Dai, Z.; Sun, Q.; Liu, X.; Bian, C.; Wu, Q.; Pan, S.; Wang, L.; Meng, X.; Deng, F.; Xiao, F.-S. Metalated porous porphyrin polymers as efficient heterogeneous catalysts for cycloaddition of epoxides with CO_2 under ambient conditions. *J. Catal.* **2016**, *338*, 202–209. [CrossRef]

22. Chen, Y.; Luo, R.; Xu, Q.; Zhang, W.; Zhou, X.; Ji, H. State-of-the-art aluminum porphyrin-based heterogeneous catalysts for the chemical fixation of CO_2 into cyclic carbonates at ambient conditions. *ChemCatChem* **2017**, *9*, 767–773. [CrossRef]

23. Zhai, G.; Liu, Y.; Lei, L.; Wang, J.; Wang, Z.; Zheng, Z.; Wang, P.; Cheng, H.; Dai, Y.; Huang, B. Light-promoted CO_2 conversion from epoxides to cyclic carbonates at ambient conditions over a Bi-based metal–organic framework. *ACS Catal.* **2021**, *11*, 1988–1994. [CrossRef]

24. Ding, M.; Jiang, H.-L. Incorporation of imidazolium-based poly (ionic liquid)s into a metal–organic framework for CO_2 capture and conversion. *ACS Catal.* **2018**, *8*, 3194–3201. [CrossRef]

25. Dai, W.; Li, Q.; Long, J.; Mao, P.; Xu, Y.; Yang, L.; Zou, J.; Luo, X. Hierarchically mesoporous imidazole-functionalized covalent triazine framework: An efficient metal-and halogen-free heterogeneous catalyst towards the cycloaddition of CO_2 with epoxides. *J. CO2 Util.* **2022**, *62*, 102101. [CrossRef]

26. Liu, F.; Duan, X.; Dai, X.; Du, S.; Ma, J.; Liu, F.; Liu, M. Metal-decorated porous organic frameworks with cross-linked pyridyl and triazinyl as efficient platforms for CO_2 activation and conversion under mild conditions. *Chem. Eng. J.* **2022**, *445*, 136687. [CrossRef]

27. Ma, P.; Ding, M.; Zhang, Y.; Rong, W.; Yao, J. Integration of lanthanide-imidazole containing polymer with metal-organic frameworks for efficient cycloaddition of CO_2 with epoxides. *Sep. Purif. Technol.* **2023**, *313*, 123498. [CrossRef]

28. Rui, Z.; Ji, H.; Lin, Y.S. Modeling and analysis of ceramic-carbonate dual-phase membrane reactor for carbon dioxide reforming with methane. *Int. J. Hydrogen Energy* **2011**, *36*, 8292–8300. [CrossRef]

29. Anderson, M.; Lin, Y.S. Carbon dioxide separation and dry reforming of methane for synthesis of syngas by a dual-phase membrane reactor. *AIChE J.* **2013**, *59*, 2207–2218. [CrossRef]

30. Pakhare, D.; Spivey, J. A review of dry (CO_2) reforming of methane over noble metal catalysts. *Chem. Soc. Rev.* **2014**, *43*, 7813–7837. [CrossRef]

31. Zhang, P.; Tong, J.; Huang, K. Combining electrochemical CO_2 capture with catalytic dry methane reforming in a single reactor for low-cost syngas production. *ACS Sustain. Chem. Eng.* **2016**, *4*, 7056–7065. [CrossRef]

32. Zhang, P.; Tong, J.; Huang, K. Dry-oxy methane reforming with mixed e(-)/CO$_3^{2-}$ conducting membranes. *ACS Sustain. Chem. Eng.* **2017**, *5*, 5432–5439.

33. Zhang, P.; Tong, J.; Huang, K. Role of CO$_2$ in catalytic ethane-to-ethylene conversion using a high-temperature CO$_2$ transport membrane reactor. *ACS Sustain. Chem. Eng.* **2019**, *7*, 6889–6897. [CrossRef]

34. Chen, T.J.; Wang, Z.G.; Liu, L.N.; Pati, S.; Wai, M.H.; Kawi, S. Coupling CO$_2$ separation with catalytic reverse water-gas shift reaction via ceramic-carbonate dual-phase membrane reactor. *Chem. Eng. J.* **2020**, *379*, 122182. [CrossRef]

35. Xing, W.; Peters, T.; Fontaine, M.-L.; Evans, A.; Henriksen, P.P.; Norby, T.; Bredesen, R. Steam-promoted CO$_2$ flux in dual-phase CO$_2$ separation membranes. *J. Membr. Sci.* **2015**, *482*, 115–119. [CrossRef]

36. Wu, H.C.; Rui, Z.B.; Lin, J.Y.S. Hydrogen production with carbon dioxide capture by dual-phase ceramic-carbonate membrane reactor via steam reforming of methane. *J. Membr. Sci.* **2020**, *598*, 117780. [CrossRef]

37. Ovalle-Encinia, O.; Wu, H.C.; Chen, T.J.; Lin, J.Y.S. CO$_2$-permselective membrane reactor for steam reforming of methane. *J. Membr. Sci.* **2022**, *641*, 119914. [CrossRef]

38. Li, X.; Huang, K.; Van Dam, N.; Jin, X. Performance projection of a high-temperature CO$_2$ transport membrane reactor for combined CO$_2$ capture and methane-to-ethylene conversion. *J. Electrochem. Soc.* **2022**, *169*, 053501.

39. Zhang, K.; Sun, S.; Huang, K. Oxidative coupling of methane (OCM) conversion into C$_2$ products through a CO$_2$/O$_2$ co-transport membrane reactor. *J. Membr. Sci.* **2022**, *661*, 120915. [CrossRef]

40. Zhang, P.; Tong, J.; Huang, K. Self-formed, mixed-conducting, triple-phase membrane for efficient CO$_2$/O$_2$ capture from flue gas and in situ dry-oxy methane reforming. *ACS Sustain. Chem. Eng.* **2018**, *6*, 14162–14169. [CrossRef]

41. Fabian-Anguiano, J.A.; Mendoza-Serrato, C.G.; Gomez-Yanez, C.; Zeifert, B.; Ma, X.; Ortiz-Landeros, J. Simultaneous CO$_2$ and O$_2$ separation coupled to oxy-dry reforming of CH$_4$ by means of a ceramic-carbonate membrane reactor for in situ syngas production. *Chem. Eng. Sci.* **2019**, *210*, 115250.

42. Fabian-Anguiano, J.A.; Ramirez-Moreno, M.J.; Balmori-Ramirez, H.; Romero-Serrano, J.A.; Romero-Ibarra, I.C.; Ma, X.; Ortiz-Landeros, J. Syngas production with CO$_2$ utilization through the oxidative reforming of methane in a new cermet-carbonate packed-bed membrane reactor. *J. Membr. Sci.* **2021**, *637*, 119607. [CrossRef]

43. Shao, B.; Zhang, Y.; Sun, Z.; Li, J.; Gao, Z.; Xie, Z.; Hu, J.; Liu, H. CO$_2$ capture and in-situ conversion: Recent progresses and perspectives. *Green Chem. Eng.* **2022**, *3*, 189–198. [CrossRef]

44. Sun, S.; Sun, H.; Williams, P.T.; Wu, C. Recent advances in integrated CO$_2$ capture and utilization: A review. *Sustain. Energy Fuels* **2021**, *5*, 4546–4559. [CrossRef]

45. Zhang, W.; Ma, D.; Pérez-Ramírez, J.; Chen, Z. Recent progress in materials exploration for thermocatalytic, photocatalytic, and integrated photothermocatalytic CO$_2$-to-fuel conversion. *Adv. Energy Sustain. Res.* **2022**, *3*, 2100169. [CrossRef]

46. Kim, S.M.; Abdala, P.M.; Broda, M.; Hosseini, D.; Copéret, C.; Müller, C. Integrated CO$_2$ capture and conversion as an efficient process for fuels from greenhouse gases. *ACS Catal.* **2018**, *8*, 2815–2823. [CrossRef]

47. Tian, S.; Yan, F.; Zhang, Z.; Jiang, J. Calcium-looping reforming of methane realizes in situ CO$_2$ utilization with improved energy efficiency. *Sci. Adv.* **2019**, *5*, eaav5077. [CrossRef]

48. Hu, J.; Hongmanorom, P.; Chirawatkul, P.; Kawi, S. Efficient integration of CO$_2$ capture and conversion over a Ni supported CeO$_2$-modified CaO microsphere at moderate temperature. *Chem. Eng. J.* **2021**, *426*, 130864. [CrossRef]

49. Wang, G.; Guo, Y.; Yu, J.; Liu, F.; Sun, J.; Wang, X.; Wang, T.; Zhao, C. Ni-CaO dual function materials prepared by different synthetic modes for integrated CO$_2$ capture and conversion. *Chem. Eng. J.* **2022**, *428*, 132110. [CrossRef]

50. Sun, H.; Wang, J.; Zhao, J.; Shen, B.; Shi, J.; Huang, J.; Wu, C. Dual functional catalytic materials of Ni over Ce-modified CaO sorbents for integrated CO$_2$ capture and conversion. *Appl. Catal. B Environ.* **2019**, *244*, 63–75. [CrossRef]

51. Duyar, M.S.; Trevino, M.A.A.; Farrauto, R.J. Dual function materials for CO$_2$ capture and conversion using renewable H$_2$. *Appl. Catal. B Environ.* **2015**, *168*, 370–376. [CrossRef]

52. Arellano-Treviño, M.A.; He, Z.; Libby, M.C.; Farrauto, R.J. Catalysts and adsorbents for CO$_2$ capture and conversion with dual function materials: Limitations of Ni-containing DFMs for flue gas applications. *J. CO2 Util.* **2019**, *31*, 143–151. [CrossRef]

53. Porta, A.; Visconti, C.G.; Castoldi, L.; Matarrese, R.; Jeong-Potter, C.; Farrauto, R.; Lietti, L. Ru-Ba synergistic effect in dual functioning materials for cyclic CO$_2$ capture and methanation. *Appl. Catal. B Environ.* **2021**, *283*, 119654. [CrossRef]

54. Bermejo-López, A.; Pereda-Ayo, B.; González-Marcos, J.; González-Velasco, J. Mechanism of the CO$_2$ storage and in situ hydrogenation to CH4. Temperature and adsorbent loading effects over Ru-CaO/Al$_2$O$_3$ and Ru-Na$_2$CO$_3$/Al$_2$O$_3$ catalysts. *Appl. Catal. B Environ.* **2019**, *256*, 117845. [CrossRef]

55. Bermejo-López, A.; Pereda-Ayo, B.; González-Marcos, J.; González-Velasco, J. Ni loading effects on dual function materials for capture and in-situ conversion of CO$_2$ to CH$_4$ using CaO or Na$_2$CO$_3$. *J. CO2 Util.* **2019**, *34*, 576–587. [CrossRef]

56. Al-Mamoori, A.; Rownaghi, A.A.; Rezaei, F. Combined capture and utilization of CO$_2$ for syngas production over dual-function materials. *ACS Sustain. Chem. Eng.* **2018**, *6*, 13551–13561. [CrossRef]

57. Duyar, M.S.; Wang, S.; Arellano-Trevino, M.A.; Farrauto, R.J. CO$_2$ utilization with a novel dual function material (DFM) for capture and catalytic conversion to synthetic natural gas: An update. *J. CO2 Util.* **2016**, *15*, 65–71. [CrossRef]

58. Garbarino, G.; Bellotti, D.; Riani, P.; Magistri, L.; Busca, G. Methanation of carbon dioxide on Ru/Al$_2$O$_3$ and Ni/Al$_2$O$_3$ catalysts at atmospheric pressure: Catalysts activation, behaviour and stability. *Int. J. Hydrogen Energy* **2015**, *40*, 9171–9182. [CrossRef]

59. Wang, S.; Schrunk, E.T.; Mahajan, H.; Farrauto, R.J. The role of ruthenium in CO_2 capture and catalytic conversion to fuel by dual function materials (DFM). *Catalysts* **2017**, *7*, 88. [CrossRef]
60. Wang, S.; Farrauto, R.J.; Karp, S.; Jeon, J.H.; Schrunk, E.T. Parametric, cyclic aging and characterization studies for CO_2 capture from flue gas and catalytic conversion to synthetic natural gas using a dual functional material (DFM). *J. CO2 Util.* **2018**, *27*, 390–397. [CrossRef]